The Astrophysical Journal Letters, 971:L34 (8pp), 2024 August 20 https://doi.org/10.3847/2041-8213/ad6990

Fragmentation in Gravitationally Unstable Collapsar Disks and Subsolar Neutron Star Mergers

Brian D. Metzger[1,2], Lam Hui[1], and Matteo Cantiello[2,3]
[1] Department of Physics and Columbia Astrophysics Laboratory, Columbia University, New York, NY 10027, USA
[2] Center for Computational Astrophysics, Flatiron Institute, 162 5th Ave., New York, NY 10010, USA
[3] Department of Astrophysical Sciences, Princeton University, Princeton, NJ 08544, USA
Received 2024 July 10; revised 2024 July 29; accepted 2024 July 31; published 2024 August 13

Abstract

Although stable neutron stars (NSs) can in principle exist down to masses $M_{\rm ns} \approx 0.1\,M_\odot$, standard models of stellar core-collapse predict a robust lower limit $M_{\rm ns} \gtrsim 1.2\,M_\odot$, roughly commensurate with the Chandrasekhar mass $M_{\rm Ch}$ of the progenitor's iron core (electron fraction $Y_e \approx 0.5$). However, this limit may be circumvented in sufficiently dense neutron-rich environments ($Y_e < 0.5$) for which $M_{\rm Ch} \propto Y_e^2$ is reduced to $\lesssim 1\,M_\odot$. Such physical conditions could arise in the black hole accretion disks formed from the collapse of rapidly rotating stars ("collapsars"), as a result of gravitational instabilities and cooling-induced fragmentation, similar to models for planet formation in protostellar disks. We confirm that the conditions to form subsolar-mass NS (ssNS) may be marginally satisfied in the outer regions of massive neutrino-cooled collapsar disks. If the disk fragments into multiple ssNSs, their subsequent coalescence offers a channel for precipitating subsolar mass LIGO/Virgo gravitational-wave mergers that does not implicate primordial black holes. The model makes several additional predictions: (1) ∼Hz frequency Doppler modulation of the ssNS-merger gravitational-wave signals due to the binary's orbital motion in the disk; (2) at least one additional gravitational-wave event (coincident within $\lesssim$hours), from the coalescence of the ssNS-merger remnant(s) with the central black hole; (3) an associated gamma-ray burst and supernova counterpart, the latter boosted in energy and enriched with *r*-process elements from the NS merger(s) embedded within the exploding stellar envelope ("kilonovae inside a supernova").

Unified Astronomy Thesaurus concepts: Neutron stars (1108); Accretion (14); Gamma-ray bursts (629); Gravitational wave sources (677)

1. Introduction

The vast majority of neutron stars (NSs) in nature are formed when the (usually predominantly, iron and nickel) core of a massive star undergoes gravitational collapse at the end of its nuclear burning evolution (e.g., Burrows & Vartanyan 2021). A minority of NSs are also likely formed from the accretion-induced collapse of white dwarfs in compact binary systems (e.g., Nomoto & Kondo 1991). In both cases, the characteristic mass of the collapsing body is set by the Chandrasekhar (1931) value:

$$M_{\rm Ch} \simeq 1.45 M_\odot \left(\frac{Y_e}{0.5}\right)^2, \quad (1)$$

where Y_e is the electron fraction, normalized to the value $Y_e \approx 0.44$–0.5 for symmetric or nearly symmetric nuclei such as ^{16}O or ^{56}Fe. In detail, the stellar core's mass at collapse differs from Equation (1) due to various corrections (e.g., finite entropy, photodisintegration and electron captures), as does the gravitational mass of the final NS (subject, e.g., to neutrino losses and the precise explosion mass cut). Nevertheless, modern supernova simulations predict NS masses in a range $\approx$1.2–1.6 $M_\odot$ (e.g., Sukhbold et al. 2016; Burrows et al. 2019; Ertl et al. 2020; Woosley et al. 2020), comparable to $M_{\rm Ch}$. The lower bound of this range is roughly compatible with the $\simeq$1.17 $M_\odot$ secondary companion in the pulsar binary PSR J0453 +1559 (Martinez et al. 2015), claimed to be the least massive NS known (e.g., Suwa et al. 2018; however, see Tauris & Janka 2019). This stands in contrast to theoretically allowed (i.e., dynamically stable) NS solutions, which extend down to masses $\approx 0.1\,M_\odot$ (e.g., Lattimer & Prakash 2004), an order of magnitude below what appears possible to create via ordinary stellar evolution.

Although no known instances of an NS weighing less than a solar mass have yet been confirmed (however, see Doroshenko et al. 2022), their potential existence in nature is of great interest. If subsolar NSs (ssNSs) are created or otherwise end up in tight stellar binaries orbiting another compact object, their resulting gravitational-wave-driven coalescence may manifest in the growing sample of compact object mergers (Mandel & Broekgaarden 2022). Based on their first three science runs, the Advanced LIGO/Virgo observatories have placed upper limits on the rate of merging subsolar compact objects with masses $\approx$0.2–1 $M_\odot$ (Abbott et al. 2018, 2022; LVK Collaboration 2023; however, see Morrás et al. 2023). The discovery of subsolar-mass mergers would seemingly have major implications for fundamental physics, insofar as it would offer arguably the cleanest evidence for the existence of primordial black holes formed at the beginning of the Universe (see Carr et al. 2021 for a review).[4] Given these high stakes, one is motivated to consider any astrophysical scenarios for creating

[4] In principle, tidal effects on the gravitational-wave form can distinguish mergers of subsolar-mass black holes from very low-mass ssNSs (Silva et al. 2016; Bandopadhyay et al. 2023; Crescimbeni et al. 2024).

and merging ssNSs, even speculative ones (e.g., Popov et al. 2007).

The majority of massive stars are believed to be rotating slowly at death, leading to NS birth following a neutrino-driven supernova explosion or to the formation of slowly spinning black holes (e.g., Fuller et al. 2019) and comparatively dim electromagnetic counterparts (e.g., Antoni & Quataert 2023). However, a small fraction, $\lesssim$1%, of massive stars appear to be rotating much faster upon collapse (Cantiello et al. 2007), giving rise to the rare population of gamma-ray bursts (GRBs; Woosley & Bloom 2006). The "collapsar" model postulates that GRBs of the so-called long-duration variety are powered by the formation of a massive torus, which orbits and feeds infalling stellar material onto a newly formed black hole at rates of up to a solar mass per second or greater (Woosley 1993; MacFadyen & Woosley 1999).

The outer regions of massive collapsar accretion disks are susceptible to instabilities driven by self-gravity (Chen & Beloborodov 2007). In analogy with models for planet formation in protostar accretion disks (e.g., Boss 1997; Lodato & Rice 2004; Chen et al. 2023) or star formation in accretion disks around supermassive black holes (e.g., Levin 2003; Goodman & Tan 2004), cooling-induced fragmentation in gravitationally unstable collapsar disks offers the potential to form self-bound objects with masses comparable to NSs. Such a scenario was proposed by Piro & Pfahl (2007), motivated by the potential of such disk-formed NSs to generate a detectable gravitational-wave signal upon coalescing with the central black hole.

In light of the renewed interest in subsolar-mass compact objects, we revisit the conditions for gravitational instability–induced fragmentation and NS formation in collapsar disks. We further consider the possibility that multiple such ssNSs formed, e.g., through the fission of self-gravitating clumps, could merge with one another prior to their coalescence with the central black hole. We highlight several predictions of this channel testable for future gravitational-wave events detected by LIGO/Virgo or its successor observatories. The envisioned scenario is summarized in Figure 1, the details of which will be fleshed out as we go along.

2. NS Mergers in Collapsar Disks

2.1. Gravitationally Unstable Collapsar Disks

We consider the core collapse of a massive $\gtrsim$20 $M_\odot$ star, which fails to explode promptly and results in the formation a black hole of mass $M_\bullet \sim 3$–30 $M_\odot$. If the star is rotating sufficiently rapidly at the time of collapse, then the infalling outer layers of its core (i.e., those with the largest angular momentum) will not directly fall into the black hole but will instead first land in a centrifugally supported torus, over timescales of seconds to minutes set by the free-fall time of the star. This torus subsequently accretes toward the black hole at a very high rate $\dot{M} \gtrsim 0.1 - 1 M_\odot\,\mathrm{s}^{-1}$, potentially powering a relativistic bipolar jet, which breaks out of the star and generates GRB emission (e.g., Woosley 1993; Gottlieb et al. 2023).

At large radii from the black hole $r \gtrsim 100 R_g$, where $R_g \equiv GM_\bullet/c^2$, the collapsar disk can become susceptible to instabilities arising due to self-gravity (e.g., Chen & Beloborodov 2007). In particular, the wavelength of the fastest growing unstable mode can fit inside the disk for values of the Toomre (1964) parameter

$$Q \equiv \frac{c_s \kappa}{\pi G \Sigma} \leqslant Q_0, \tag{2}$$

where $Q_0 \approx 1$–2 (e.g., Lodato & Rice 2004). Here, Σ and $\kappa \simeq \Omega \approx (GM_\bullet/r^3)^{1/2}$ are the local surface density and epicyclic/orbital frequency of the disk; c_s and $h \simeq c_s/\Omega \ll r$ are the midplane sound speed and vertical scale height. Condition (2) can be written as a lower limit on the local disk mass:

$$M_d \equiv 2\pi r^2 \Sigma > \frac{2}{Q_0}\frac{h}{r} M_\bullet. \tag{3}$$

Vertical hydrostatic equilibrium of the disk requires

$$h \simeq \frac{2P}{\Sigma \Omega^2}, \tag{4}$$

where $P(\rho, T, Y_e) = \rho c_s^2$ is the midplane pressure, which depends on the temperature T, density $\rho \simeq \Sigma/2h$, and electron fraction Y_e. The pressure includes contributions from photons, ions, and electrons/positrons; the latter are typically mildly relativistic and mildly degenerate for the conditions of interest.

The midplane pressure, and hence the disk aspect ratio h/r, is determined by the balance between heating and cooling. The primary source of heating, at least prior to the formation of any embedded compact objects, is dissipation associated with shear viscosity. This occurs at a specific rate:

$$\dot{q}_+ \approx \nu \left(\frac{d\Omega}{d \ln r}\right)^2 \approx \frac{9}{4}\alpha r^2 \Omega^3 \left(\frac{h}{r}\right)^2, \tag{5}$$

where we employ the Shakura & Sunyaev (1973) parameterization $\nu = \alpha c_s h \approx \alpha r^2 \Omega (h/r)^2$ with $\alpha < 1$, a dimensionless parameter.

While the inner regions of collapsar disks can be opaque to thermal neutrino emission, the disk is transparent to neutrinos at the larger radii where gravitational instabilities operate. The disk is also generally sufficiently hot ($kT \gtrsim 1$ MeV) that heavy elements from the infalling star (e.g., ^{4}He) at least partially dissociate into free neutrons and protons. The dominant neutrino-cooling mechanism under these conditions is the capture of electrons or positrons onto the free nucleons,

$$e^- + p \rightarrow \nu_e + n; \;\; e^+ + n \rightarrow \bar{\nu}_e + p, \tag{6}$$

which provide a total specific cooling rate:

$$\dot{q}_- = \dot{q}_{e^- p} + \dot{q}_{e^+ n}. \tag{7}$$

Additional cooling can occur from helium dissociation (Piro & Pfahl 2007) though we neglect this process here for simplicity and return to its effect later on.

The processes (Equation (6)) not only cool the disk but can change the ratio of protons to neutrons, i.e., the electron fraction Y_e, from the symmetric initial composition $Y_{e,0} \simeq 0.5$ of the infalling stellar material (e.g., Siegel et al. 2019). Again neglecting neutrino absorptions, these weak interactions act to drive Y_e to an equilibrium value:

$$Y_{e,\mathrm{eq}} \simeq \frac{\lambda_{e^+ n}}{\lambda_{e^- p} + \lambda_{e^+ n}}, \tag{8}$$

where $\lambda_{e^-\mathrm{p}}(T, \rho, Y_e) \equiv n_{e^-} \langle \sigma_{e^-\mathrm{p}} v_{e^-} \rangle$ and $\lambda_{e^+\mathrm{n}}(T, \rho, Y_e) \equiv n_{e^+} \langle \sigma_{e^+\mathrm{n}} v_{e^+} \rangle$ are the rates of electron and

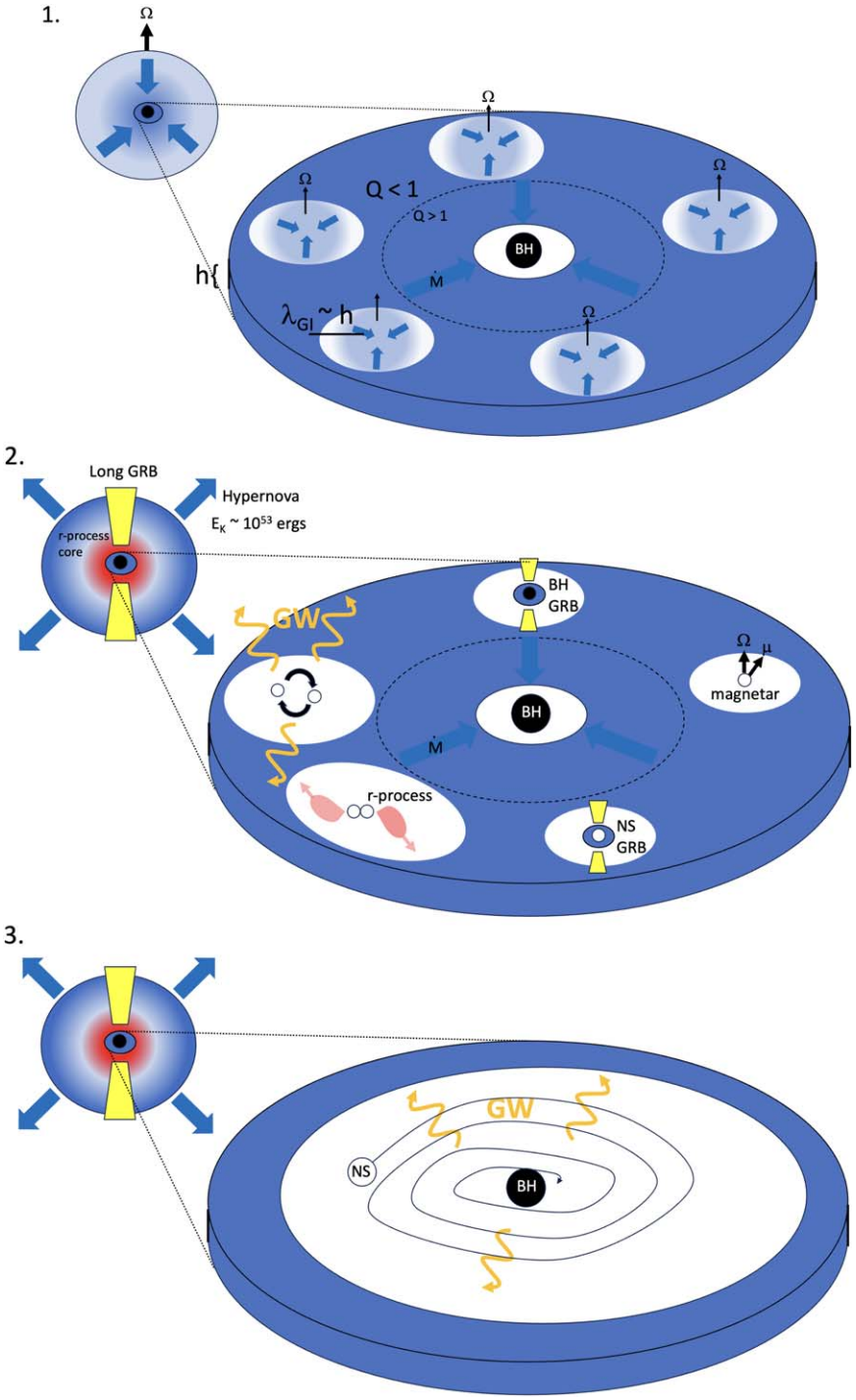

Figure 1. Schematic illustration of the stages of the presented model: (1) core collapse of a massive rotating star, generating an accretion disk that feeds the central black hole at a high rate $\dot{M} \gtrsim M_\odot\ \mathrm{s}^{-1}$. Subsequent fragmentation of the disk at radii $R_\mathrm{d} \gtrsim 100R_\mathrm{g}$ where $Q \lesssim Q_0 \sim 1$ leads to the collapse and formation of gravitationally bound compact objects, potentially including tight binaries containing subsolar-mass NSs; (2) binary mergers of the NSs formed within the disk lead to LIGO/Virgo-band gravitational-wave coalescence events, *r*-process mass ejection, and the creation of energetic compact merger remnants, potentially including accreting black holes and millisecond magnetars (the ordinarily discussed central engines of short GRBs). Along with the disk winds and relativistic jet associated with accretion onto the central black hole, these processes feed energy and *r*-process elements into the unbound ejecta shell from the exploding star; (3) the remaining compact remnant(s), potentially following a chain of hierarchical merging, inspiral into the central black hole, producing a final merger in the LIGO/Virgo band.

positron captures (Equation (6)), where σ is the relevant cross section. The inner regions of collapsar disks are sufficiently dense that electrons are degenerate; this suppresses positron formation despite the high temperatures $kT \gtrsim 2m_ec^2$, such that $\lambda_{e^+n} \lesssim \lambda_{e^-p}$, and hence, $Y_{e,\mathrm{eq}} < 0.5$ (e.g., Beloborodov 2003; Metzger et al. 2008b). Such "neutronization" of the inflowing gas may have sufficient time to occur provided the electron capture time $t_\mathrm{n} \equiv \lambda_{e^-p}^{-1}$ is shorter than the local accretion time $t_\mathrm{acc} = M_\mathrm{d}/\dot{M}$, where $\dot{M} \simeq 3\pi\nu\Sigma$ is the accretion rate.

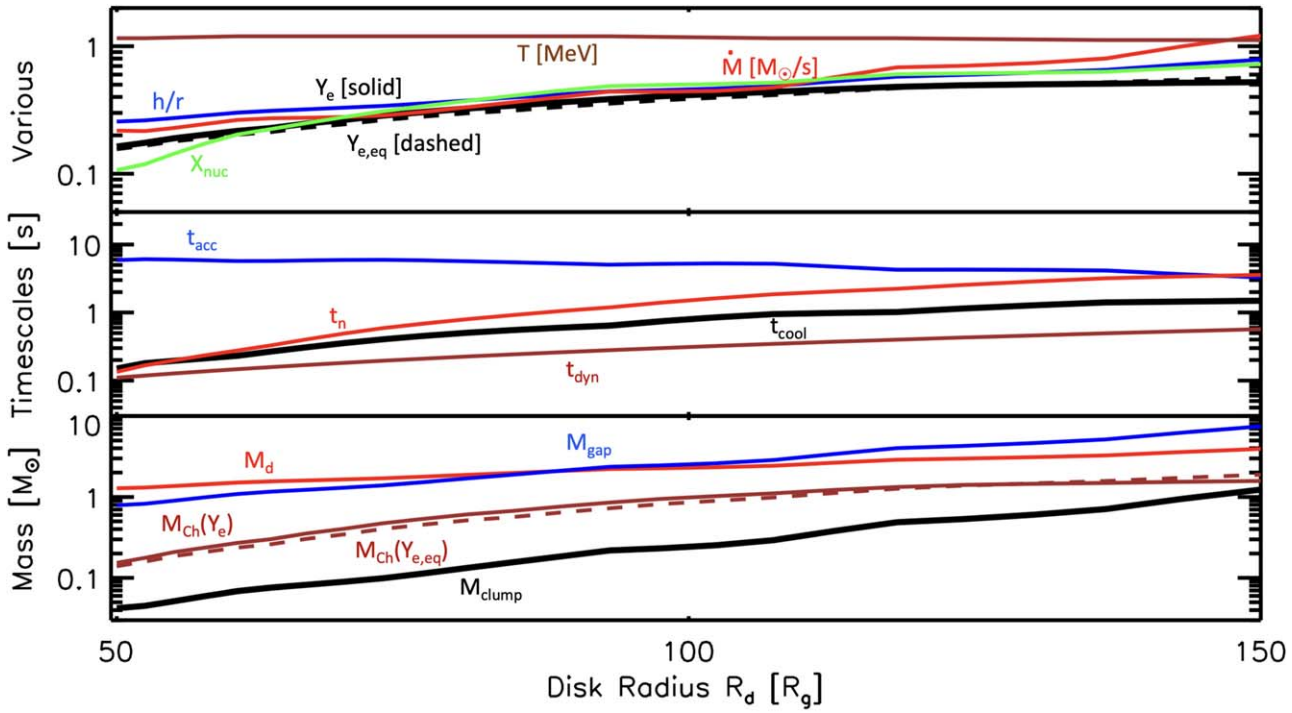

Figure 2. Properties of marginally Toomre-stable ($Q = 1.5 \approx Q_0$) collapsar disks as a function of the radius of the disk annulus $r = R_{\rm d}$ for an assumed central black hole mass $M_\bullet = 10\,M_\odot$ and viscosity $\alpha = 0.03$. Top panel: estimated electron fraction Y_e after one accretion time (Equation (9); black solid) and equilibrium electron fraction $Y_{e,\rm eq}$ (Equation (8); black dashed); disk aspect ratio h/r (blue); midplane temperature T (brown); free nucleon mass-fraction $X_{\rm nuc}$ (green); accretion rate $\dot{M}$ (red). Middle panel: neutrino-cooling time $t_{\rm cool}$ (black); dynamical/orbital time $t_{\rm dyn} = 2\pi/\Omega$ (brown); neutronization timescale $t_{\rm n} = \lambda_{e^-p}^{-1}$ (red); accretion time $t_{\rm acc}$ (blue). Bottom panel: local disk mass $M_{\rm d} = 2\pi R_{\rm d}^2\Sigma$ (red); characteristic mass of the gravitationally unstable region $M_{\rm clump} = \pi h^2\Sigma$ (black); Chandrasekhar mass $M_{\rm Ch}$, shown separately for the estimated disk electron fraction Y_e (solid brown) and for the equilibrium electron fraction $Y_{e,\rm eq}$ (dashed brown); gap opening mass $M_{\rm gap}$ (blue), above which a bound clump is sufficiently massive to open a gap within the disk.

2.2. Conditions for Disk Fragmentation and ssNS Formation

Figure 2 shows several of the above-described physical quantities for marginally Toomre-unstable ($Q \approx Q_0 = 1.5$) accretion onto a black hole of mass $M_\bullet = 10\ M_\odot$ for an effective viscosity $\alpha = 0.03$ typical of the those provided by the magnetorotational instability (Davis et al. 2010) or the maximum stress provided by gravitoturbulence in gravitationally unstable disks (Gammie 2001; Rice et al. 2005). For different assumed radii of the disk annulus $r = R_{\rm d}$, we enforce hydrostatic balance (Equation (4)) and thermal equilibrium ($\dot{q}^+ = \dot{q}^-$; Equations (5), (7)), using standard expressions for the equation of state, pair-capture rate, and associated neutrino-cooling rates (e.g., Beloborodov 2003) for an ideal gas of photons, free nucleons, alpha particles, electrons, and positrons allowing for arbitrary degrees of degeneracy and relativism.

The disk structure depends on the electron fraction, which in turn depends on the efficacy of weak interactions. Following the discussion at the end of Section 2.1 we approximate the disk electron fraction as

$$Y_e = Y_{e,0}(1 - e^{-t_{\rm n}/t_{\rm acc}}) + Y_{e,\rm eq}e^{-t_{\rm n}/t_{\rm acc}}, \quad (9)$$

where $Y_{e,0} = 0.5$ is the initial electron fraction of the disk from the infalling stellar material and $Y_{e,\rm eq}$ (Equation (8)) is the equilibrium value attained if the pair-capture reactions (6) come into equilibrium ($t_{\rm n} \ll t_{\rm acc}$).

Figure 2 shows that the collapsar disk must be massive $M_{\rm d} \gtrsim M_\odot$ with a high accretion rate $\dot{M} \gtrsim 0.5 M_\odot\ {\rm s}^{-1}$ to become gravitationally unstable. These properties are consistent with those achieved by the collapse of rapidly spinning, very massive stars $\gtrsim 30\ M_\odot$ for which the gravitational free-fall time of the helium core is typically tens of seconds (e.g., Siegel et al. 2019). For $R_{\rm d} \sim 100 R_{\rm g}$, the disk is moderately geometrically thin as a result of neutrino cooling ($h/r \sim 0.3$) with a characteristic midplane temperature $kT \approx 1$ MeV (top panel of Figure 2). The latter varies only weakly with $R_{\rm d}$ because of the sensitive temperature dependence of the neutrino-cooling rate ($\dot{q}_- \propto T^6$, roughly). The composition is partially free nucleons $X_{\rm nuc} \gtrsim 0.3$, with the remaining mass $X_{\rm He} \simeq 1$–$X_{\rm nuc}$ mostly in alpha particles.

Pair captures favor driving the disk to a neutron-rich composition $Y_{e,\rm eq} < 0.5$ for small disk sizes $R_{\rm d} \lesssim 100 R_{\rm g}$ as a result of the higher electron degeneracy that accompanies the greater density of smaller disks. Furthermore, the timescale for electron captures is sufficiently short relative to the accretion timescale ($t_{\rm n} \lesssim t_{\rm acc}$) so that the disk matter has time to become appreciably neutron rich before flowing inwards to the black hole ($Y_e \approx Y_{e,\rm eq} < 0.5$). In fact, the timescale for neutronization is only moderately longer than the dynamical or cooling timescales $t_{\rm n} \sim t_{\rm cool}$, $t_{\rm dyn}$ for small $R_{\rm d}$. As described below, this has important consequences for the minimum masses of any NS formed.

The disk being gravitationally unstable does not guarantee that the resulting overdensities will fragment into gravitationally bound bodies ("clumps") nor that such clumps would continue to contract to become NSs. For NS formation to occur, at least two conditions must be satisfied:

1. The protoclumps must cool radiatively faster than they are sheared apart by the mean flow, i.e., (Gammie 2001)

$$t_{\rm cool}/t_{\rm dyn} \lesssim \mathcal{O}(1) \quad (10)$$

must be satisfied, where $t_{\rm dyn} \equiv 2\pi/\Omega$ and $t_{\rm cool} \equiv e_{\rm th}/(\rho \dot{q}^-)$ are the dynamical/orbital and radiative cooling time, respectively, and $e_{\rm th}$ is the thermal energy density. The precise order-unity threshold on the right side of Equation (10) is uncertain in the present context, as it depends on the equation of state and cooling function of the disk and must be ascertained with hydrodynamical simulations (e.g., Rice et al. 2005; Chen et al. 2023).

2. To form an NS, the mass of the collapsing self-bound clump must exceed the Chandrasekhar mass (Equation (1)), i.e.,

$$M_{\rm clump} \gtrsim M_{\rm Ch}(Y_e). \tag{11}$$

This way, even once thermal pressure is radiated away, electron degeneracy pressure is unable to support the clump, enabling its continued collapse to nuclear densities.

The first condition (Equation (10)) is at best marginally satisfied in the initial disk state for our example solution, for which $t_{\rm cool} \sim t_{\rm dyn}$ (middle panel of Figure 2). However, since the neutrino-cooling rate increases with temperature ($t_{\rm cool} \propto T^{-2}\rho^{-1}$, roughly) as a marginally bound region of the disk is compressed to higher densities (roughly adiabatically, $\rho \propto T^{1/3}$), then the ratio $t_{\rm cool}/t_{\rm dyn} \propto \rho^{-11/6}$ becomes shorter as the collapse proceeds, where $t_{\rm dyn} \propto \rho^{-1/2}$ is now the free-fall time of the clump. The additional cooling available from further alpha-particle dissociation during the collapse, of up to $Q_\alpha(1 - X_{\rm nuc}) \gtrsim 3\,{\rm MeV}$ per nucleon $\gtrsim kT$ (where $Q_\alpha \simeq 7\,{\rm MeV}$ per nucleon is the total energy release per dissociated alpha particle), strengthens this conclusion.

Furthermore, in cases where the disk grows via infall from a surrounding stellar envelope (as may describe the collapsar case), the fragmentation criterion may be more nuanced (Kratter & Lodato 2016). The maximum level of angular momentum transport (i.e., the effective value of "α") set by gravitoturbulence depends on the disk properties, which in turn depend on the balance between infall from the stellar envelope adding mass to the disk and accretion depleting it. For an isothermal disk, Kratter et al. (2010) show that fragmentation to form a binary or multiple system occurs above a minimum mass-infall rate, which can be expressed as

$$\dot{M} > \dot{M}_{\rm K} \equiv K \frac{(c_s^3/G)^{5/3}}{(M_\bullet \Omega)^{2/3}} \approx 65 M_\odot\ {\rm s}^{-1} \times \left(\frac{K}{90}\right)\left(\frac{kT}{1\,{\rm MeV}}\right)^{5/2}\left(\frac{R_{\rm d}}{100 R_{\rm g}}\right), \tag{12}$$

where in the second line, we have approximated the disk's midplane sound speed $c_s \approx (kT/m_p)^{1/2}$, assuming ion pressure dominates. Applying the prefactor $K \approx 90$ found empirically by Kratter et al. (2010), the required values $\dot{M}_{\rm K} \sim 10 - 100 M_\odot\ {\rm s}^{-1}$ are unphysically large, except perhaps for the most massive collapsing stars $\gtrsim 100\ M_\odot$ (Siegel et al. 2022). On the other hand, collapsar disks are not isothermal, and other physical processes like α particle dissociation cooling may come into play, motivating additional simulation work in the present context to arrive at a definitive conclusion regarding fragmentation.

Regarding the second condition (Equation (11)), the initial mass of the gravitationally bound clumps may be crudely estimated by the disk's mass enclosed within a region of radius equal to the maximum Toomre-unstable wavelength $\sim h$, i.e.,

$$M_{\rm clump} \simeq \pi h^2 \Sigma. \tag{13}$$

Our solutions find $M_{\rm clump} \sim 0.03$–$1\ M_\odot$ across the disk radii of interest, typically several times smaller than $M_{\rm ch}$. Although Equation (11) is not initially satisfied (in this example), it may become so at a later stage. First, the electron fraction (and hence $M_{\rm Ch}$) will continue to decrease from its initial value at the time of fragmentation, as the temperature of a collapsing clump rises, shortening the timescale for electron captures (roughly as $t_{\rm n} \propto T^{-5}$).

Second, any gravitationally bound clumps can continue to grow over several orbits, e.g., as a result of mergers with other clumps or gas accretion. A bound object is only sufficiently massive to open a gap in the disk, above a critical mass that is frequently approximated as (e.g., Crida et al. 2006)

$$M_{\rm gap} \approx \frac{50 \nu M_\bullet}{R_{\rm d}^2 \Omega}. \tag{14}$$

The fact that $M_{\rm gap} \sim 1$–$10\ M_\odot$ across the range of $R_{\rm d}$ exceeds the clump mass (Figure 2) makes a gap opening unlikely. This implies that gravitationally bound clumps can in principle grow through mergers with other clumps located at the same annulus in the disk (or, potentially, through gas accretion) to masses $\gtrsim M_{\rm Ch}$ capable of collapse. Once forming, however, an NS may not continue to grow appreciably due to the powerful feedback that supercritical accretion has on the growth rate of a compact object (e.g., Blandford & Begelman 1999).

In summary, while there are many uncertainties, we conclude that collapsar disks are plausibly capable of (a) becoming gravitationally unstable; (b) fragmenting into bound objects as a result of neutrino cooling and alpha dissociation; and (c) producing fragments which, either initially, or through subsequent accretion and/or contraction/neutronization, exceed the Chandrasekhar mass $M_{\rm Ch} \propto Y_e^2$ and thus can collapse to NSs, (d) the latter potentially with subsolar masses due to the neutron-rich composition of the electron-degenerate disk and fragments, $Y_e \lesssim 0.5$. These conditions for creating ssNSs are generally satisfied for massive disks $\gg M_\odot$ formed with large sizes $R_{\rm d} \sim 100 R_{\rm g}$ (see also Piro & Pfahl 2007).

2.3. Binary NS Formation and Hierarchical Mergers Thereafter

Once the collapse of a bound clump with mass $\gtrsim M_{\rm Ch}$ is underway, its subsequent evolution will qualitatively resemble the final stages of the core collapse of a massive star. The collapse process will unfold on the free-fall time of the clump, which equals the disk's dynamic timescale $t_{\rm dyn} \lesssim$ seconds (Figure 2). The final phase as the proto-NS undergoes Kelvin–Helmholtz contraction to a radius $R_{\rm ns} \lesssim 20\,{\rm km}$ takes place on a similar timescale of a few seconds (Burrows & Lattimer 1986).

However, one potentially significant barrier to collapse is the large, specific angular momentum of the clump $j_{\rm clump} \sim h(\delta v) \approx h^2\Omega$ (where $\delta v \sim h\Omega$ is the velocity shear across the clump), which generally exceeds the maximum rotational angular momentum of an NS, $j_{\rm max} \lesssim (R_{\rm ns} G M_{\rm ns})^{1/2}$, by a factor of several. One way that this barrier could be overcome is if a collapsing fragment fissions into one or more sub-bodies, placing its excess angular momentum into orbital motion (see

Colpi & Rasio 1994 and Colpi & Wasserman 2002 for related early ideas in the context of NS mergers and core-collapse supernovae, respectively).[5] Fluid simulations by Alexander et al. (2008) are broadly supportive of this possibility though additional studies are needed. Equating $j_{\rm clump}$ to the orbital angular momentum $j_{\rm orb} = (2GM_{\rm ns}a_{\rm bin})^{1/2}$ of a binary of two equal mass NSs gives an estimate of the binary separation:

$$a_{\rm bin} = \frac{R_{\rm d}}{2}\frac{M_\bullet}{M_{\rm ns}}\left(\frac{h}{r}\right)^4 \approx 120\ {\rm km}\left(\frac{R_{\rm d}}{100R_{\rm g}}\right) \times \left(\frac{M_{\rm ns}}{0.5M_\odot}\right)^{-1}\left(\frac{M_\bullet}{10M_\odot}\right)^{2}\left(\frac{M_{\rm d}}{0.3M_\bullet}\right)^{4}, \quad (15)$$

where we have used Equation (3) for $Q = Q_0 = 2$. We note that $a_{\rm bin} < r_{\rm H}$ for fiducial parameters, i.e., the putative NS binary fits within its Hill sphere.

Neglecting any additional sources of binary tightening (e.g., due to torques from the surrounding gas disk; Stone et al. 2017), the newly formed NS binary will merge through gravitational-wave emission on a timescale:

$$\tau_{\rm NS-NS} \simeq \frac{5}{512}\frac{c^5 a_{\rm bin}^4}{G^3 M_{\rm ns}^3} \simeq 17\ {\rm s}\left(\frac{a_{\rm bin}}{120\ {\rm km}}\right)^4\left(\frac{M_{\rm ns}}{0.5M_\odot}\right)^{-3}. \quad (16)$$

Aside from their potential to involve subsolar-mass bodies, this gravitational-wave signal may be unique in other ways from most other NS mergers in nature (e.g., those formed through binary star evolution). Insofar that $\tau_{\rm NS-NS}$ is longer than the orbital time of the binary around the central black hole $t_{\rm dyn} \sim 0.1$–1 s (Figure 2), the early stages of the chirp as viewed by an external observer would be subject to Doppler modulation, at a frequency $f_{\rm orb} \sim 1/t_{\rm dyn} \sim 1$–10 Hz. This effect on the gravitational-wave form may be detectable with LIGO/Virgo in some events (e.g., Meiron et al. 2017). We might also expect the frequency of the orbital modulation of the gravitational-wave signal to be anticorrelated with the mass of the NS binary since $M_{\rm clump}$ and $M_{\rm Ch}$ typically increase with $R_{\rm d}$. We also note that if $\tau_{\rm NS-NS}$ is sufficiently short, then the merging proto-NSs may still be inflated from their formation process, with radii larger than in their asymptotic cold state; this could improve the prospects for detecting tidal effects in the gravitational-wave form (e.g., Bandopadhyay et al. 2023).

The end product of the merger of an NS is a compact remnant, either a black hole or NS, depending primarily on the total mass of the binary (e.g., Margalit & Metzger 2019). Although this merger product will subsequently release enormous energy, mostly in the form of roughly axisymmetric electromagnetic outflows (Section 2.4), neither these—nor the recoil kick received from the gravitational waves—are likely to be sufficient to unbind the merger product from the potential well of the central black hole (the escape speed at $\lesssim 200R_{\rm g}$ is $\gtrsim 0.1c$). This implies that if multiple fragments form and collapse to NS(s) at separate locations in the disk, hierarchical mergers between these objects can take place, similar to those envisioned to occur between binary black holes in dense stellar environments (e.g., Gerosa & Berti 2017). On the other hand, strong gravitational interactions between compact objects that do not lead to mergers could result in a solitary ssNS as a result of a large kick that unbinds the star from the disk. Such a body would only likely be detectable (or, at least, be identifiable as a low-mass NS) if it were to somehow end up in a binary system. Such a match is unlikely to take place in the field but could in principle take place for core-collapse events in dense stellar environments such as galactic nuclei (e.g., Jermyn et al. 2022).

Regardless of the prolificity of collapsar disks, the final products of any such merger chain must eventually merge with the central black hole (Piro & Pfahl 2007). If such high mass-ratio inspiral(s), which begin from an initial separation $a_{\rm bin} \sim R_{\rm d} \sim 100R_{\rm g}$ corresponding to the fragmentation radius, are also driven exclusively by gravitational waves, then the delay of the merger time with respect to the associated earlier in-disk mergers is given by

$$\tau_{\rm BH-NS} \simeq \frac{5}{256}\frac{c^5 R_{\rm d}^4}{G^3 M_\bullet^2 (2M_{\rm ns})} \approx 10^3\ {\rm s} \times \left(\frac{R_{\rm d}}{100R_{\rm g}}\right)^4\left(\frac{M_{\rm ns}}{0.5M_\odot}\right)^{-1}\left(\frac{M_\bullet}{10M_\odot}\right)^{2}, \quad (17)$$

i.e., minutes to hours, depending sensitively on the details of the system. Type II migration in the gaseous disk may lead to faster migration, causing observable deviation from the vacuum gravitational-wave signal (Piro & Pfahl 2007). Aside from the compact merger signals described above, regions of the disk that do not cool efficiently to fragment into bound remnants can also generate a quasiperiodic gravitational-wave signal as the result of spiral density waves (e.g., Siegel et al. 2022) or trapped Rossby waves (Gottlieb et al. 2024).

2.4. Electromagnetic Counterparts: Kilonovae-embedded Collapsars

The above-described processes take place over a window of at most days, embedded within the environment of an exploding star. Even if the initial stellar core collapse failed to produce a successful explosion, outflows from the black hole accretion disk and relativistic jet are sufficient to power the ejection of several solar masses of material at high velocities $v \gtrsim 0.1c$ (e.g., MacFadyen & Woosley 1999), explaining the observed coincidence of energetic ("broad-lined") supernovae in association with most long GRBs (e.g., Woosley & Bloom 2006). The discovery of a long GRB or supernova following the gravitational-wave trigger from a compact object merger would thus be a smoking gun prediction of the scenario.

The presence of NS merger(s) within the collapsar disk would have several implications for the observable appearance of the associated supernovae. Neutron-rich material released during the merger process create heavy *r*-process elements (e.g., Freiburghaus et al. 1999), most of which is ejected from the binary with sufficiently high velocities ~ 0.1–$0.3c$ to become unbound from the collapsar disk. Radioactive decay within these ejecta will likely not power the cleanly observable kilonova signal seen from normal binary NS mergers (Metzger et al. 2010) because of the dense, opaque surroundings of the exploding star. However, the presence of heavy *r*-process elements in the collapsar ejecta can still impact the light curves and spectra of the supernova as a result of the high opacities of lanthanide/actinide elements relative to ordinary supernova ejecta (e.g., Siegel et al. 2019; Barnes & Metzger 2022; Patel et al. 2024).

[5] A similar process has been proposed to form Kuiper Belt binaries such as Ultima Thule within the Sun's protoplanetary disk (e.g., Nesvorný et al. 2010).

Insofar as the merger of two ssNSs will create a final remnant of mass $\lesssim 2\,M_{\odot}$, less than the Tolman–Oppenheimer–Volkoff limit, the merger will form a stable NS rather than a black hole. Such an NS remnant is necessarily very rapidly spinning (e.g., Radice et al. 2018) and likely strongly magnetized, i.e., a "millisecond magnetar" (e.g., Metzger et al. 2008a; Combi & Siegel 2023; Kiuchi et al. 2024). After forming, the magnetar will undergo rapid magnetic dipole braking, releasing a large fraction of its $\sim 10^{52}$–10^{53} erg of rotational energy into the environment in the form of a magnetized wind over a timescale of minutes to hours (e.g., Bucciantini et al. 2012; Metzger & Piro 2014). Though expanding at relativistic speeds, the magnetar wind will likely be trapped within and hence share its energy with the surrounding expanding supernova ejecta on large scales. This could substantially boost the energetics of the merger-embedded supernovae, even compared to the "hypernovae" that accompany ordinary (i.e., nonmerger hosting) collapsars.

3. Summary

The standard of evidence for treating the future detection of subsolar-mass compact objects as evidence for new physics, such as the existence of primordial black holes, must be very high. On the other hand, the number of plausible astrophysical channels for creating (much less merging) subsolar-mass compact objects is very limited. Motivated by this tension, we have outlined an admittedly speculative scenario for forming and merging ssNSs in a single environment: the gaseous accretion disks created by the collapse of massive rotating stars. The described scenario supports and expands on earlier work by Piro & Pfahl (2007).

Although our estimates paint a plausible story, a number of uncertainties remain, particularly with regards to (a) whether the stripped progenitor stars of collapsars can possess sufficient angular momentum to create massive $\gtrsim M_{\odot}$ disks at large radii $\gtrsim 100 R_{\rm g}$ around the central black hole; (b) whether the criterion for forming gravitationally bound objects is in fact satisfied by a combination of neutrino and alpha-particle dissociation cooling in a full multidimensional turbulent disk environment; (c) the resulting mass spectrum of the bound clumps, and whether clump-fissioning or gas-aided capture leads to binary NS formation; (d) the evolution of the disk electron fraction due to pair captures prior and during gravitational collapse, and how this impacts the masses of the NSs that form; and (e) feedback effects on the disk mass and energy budget from accretion onto the collapsed remnants. Some of these issues are directly amenable to numerical simulations and will be pursued in future work.

Given the uncertainties, we have emphasized a number of testable predictions of the proposed scenario:

1. *Doppler modulation of the NS-merger gravitational-wave form due to the binary's orbital motion around the central black hole*. Tidal effects may also be stronger than than predicted by the cold equation of state due to the inflated radii of newly formed NSs (the cold radii of ssNSs and associated tidal deformability being already much larger than ordinary NSs; e.g., Bandopadhyay et al. 2023).
2. *The potential for multiple hierarchical mergers over a short window of minutes to hours*. At least one final coalescence event, likely coincident within hours to days, from the merger product and the central black hole is particularly challenging to avoid (Piro & Pfahl 2007). Insofar that multiple unrelated mergers within such a short time frame from the same region of the sky and luminosity distance are likely to be rare, this prediction seems eminently testable with LIGO/Virgo or future more sensitive gravitational-wave observatories, particularly those which will provide adequate sky localization.
3. *A series of bright electromagnetic counterparts in the form of a GRB jet and its multiwavelength afterglow fed by accretion onto the black hole, followed over weeks to months by a supernova from the disk wind–aided explosion*. The explosion may be boosted in its kinetic energy and enriched in *r*-process elements from the embedded NS merger(s), the latter of which can be tested by late-time observations that probe the inner layers of the supernova ejecta (e.g., Rastinejad et al. 2024; Anand et al. 2024).

Acknowledgments

We thank the reviewer for insightful comments that improved the Letter. L.H. thanks Toni Riotto for helpful conversations. B.D.M. thanks Morgan May for helpful comments on the manuscript. B.D.M. was supported in part by the National Science Foundation (grant No. AST-2009255) and by the NASA Fermi Guest Investigator Program (grant No. 80NSSC22K1574). L.H. acknowledges support by the DOE DE-SC011941 and a Simons Fellowship in Theoretical Physics. The Flatiron Institute is supported by the Simons Foundation. This research was supported in part by grant No. NSF PHY-2309135 to the Kavli Institute for Theoretical Physics (KITP).

ORCID iDs

Brian D. Metzger https://orcid.org/0000-0002-4670-7509
Lam Hui https://orcid.org/0000-0002-4670-7509
Matteo Cantiello https://orcid.org/0000-0002-8171-8596

References

Abbott, B. P., Abbott, R., Abbott, T. D., et al. 2018, PhRvL, 121, 231103
Abbott, R., et al. 2022, PhRvL, 129, 061104
Alexander, R. D., Armitage, P. J., & Cuadra, J. 2008, MNRAS, 389, 1655
Anand, S., Barnes, J., Yang, S., et al. 2024, ApJ, 962, 68
Antoni, A., & Quataert, E. 2023, MNRAS, 525, 1229
Bandopadhyay, A., Reed, B., Padamata, S., et al. 2023, PhRvD, 107, 103012
Barnes, J., & Metzger, B. D. 2022, ApJL, 939, L29
Beloborodov, A. M. 2003, ApJ, 588, 931
Blandford, R. D., & Begelman, M. C. 1999, MNRAS, 303, L1
Boss, A. P. 1997, Sci, 276, 1836
Bucciantini, N., Metzger, B. D., Thompson, T. A., & Quataert, E. 2012, MNRAS, 419, 1537
Burrows, A., & Lattimer, J. M. 1986, ApJ, 307, 178
Burrows, A., Radice, D., & Vartanyan, D. 2019, MNRAS, 485, 3153
Burrows, A., & Vartanyan, D. 2021, Natur, 589, 29
Cantiello, M., Yoon, S. C., Langer, N., & Livio, M. 2007, A&A, 465, L29
Carr, B., Kohri, K., Sendouda, Y., & Yokoyama, J. 2021, RPPh, 84, 116902
Chandrasekhar, S. 1931, ApJ, 74, 81
Chen, W.-X., & Beloborodov, A. M. 2007, ApJ, 657, 383
Chen, Y.-X., Jiang, Y.-F., Goodman, J., & Ostriker, E. C. 2023, ApJ, 948, 120
Colpi, M., & Rasio, F. A. 1994, MmSAI, 65, 379
Colpi, M., & Wasserman, I. 2002, ApJ, 581, 1271
Combi, L., & Siegel, D. M. 2023, PhRvL, 131, 231402
Crescimbeni, F., Franciolini, G., Pani, P., & Riotto, A. 2024, PhRvD, 109, 124063
Crida, A., Morbidelli, A., & Masset, F. 2006, Icar, 181, 587

Davis, S. W., Stone, J. M., & Pessah, M. E. 2010, ApJ, 713, 52
Doroshenko, V., Suleimanov, V., Pühlhofer, G., & Santangelo, A. 2022, NatAs, 6, 1444
Ertl, T., Woosley, S. E., Sukhbold, T., & Janka, H. T. 2020, ApJ, 890, 51
Freiburghaus, C., Rosswog, S., & Thielemann, F. 1999, ApJ, 525, L121
Fuller, J., Piro, A. L., & Jermyn, A. S. 2019, MNRAS, 485, 3661
Gammie, C. F. 2001, ApJ, 553, 174
Gerosa, D., & Berti, E. 2017, PhRvD, 95, 124046
Goodman, J., & Tan, J. C. 2004, ApJ, 608, 108
Gottlieb, O., Jacquemin-Ide, J., Lowell, B., Tchekhovskoy, A., & Ramirez-Ruiz, E. 2023, ApJL, 952, L32
Gottlieb, O., Levinson, A., & Levin, Y. 2024, arXiv:2406.19452
Jermyn, A. S., Dittmann, A. J., McKernan, B., Ford, K. E. S., & Cantiello, M. 2022, ApJ, 929, 133
Kiuchi, K., Reboul-Salze, A., Shibata, M., & Sekiguchi, Y. 2024, NatAs, 8, 298
Kratter, K., & Lodato, G. 2016, ARA&A, 54, 271
Kratter, K. M., Matzner, C. D., Krumholz, M. R., & Klein, R. I. 2010, ApJ, 708, 1585
Lattimer, J. M., & Prakash, M. 2004, Sci, 304, 536
Levin, Y. 2003, arXiv:astro-ph/0307084
Lodato, G., & Rice, W. K. M. 2004, MNRAS, 351, 630
LVK Collaboration 2023, MNRAS, 526, 6234
MacFadyen, A. I., & Woosley, S. E. 1999, ApJ, 524, 262
Mandel, I., & Broekgaarden, F. S. 2022, LRR, 25, 1
Margalit, B., & Metzger, B. D. 2019, ApJL, 880, L15
Martinez, J. G., Stovall, K., Freire, P. C. C., et al. 2015, ApJ, 812, 143
Meiron, Y., Kocsis, B., & Loeb, A. 2017, ApJ, 834, 200
Metzger, B. D., Arcones, A., Quataert, E., & Martínez-Pinedo, G. 2010, MNRAS, 402, 2771
Metzger, B. D., & Piro, A. L. 2014, MNRAS, 439, 3916
Metzger, B. D., Quataert, E., & Thompson, T. A. 2008a, MNRAS, 385, 1455
Metzger, B. D., Thompson, T. A., & Quataert, E. 2008b, ApJ, 676, 1130
Morrás, G., Nuño Siles, J. F., García-Bellido, J., et al. 2023, PDU, 42, 101285
Nesvorný, D., Youdin, A. N., & Richardson, D. C. 2010, AJ, 140, 785
Nomoto, K., & Kondo, Y. 1991, ApJL, 367, L19
Patel, A., Goldberg, J. A., Renzo, M., & Metzger, B. D. 2024, ApJ, 966, 212
Piro, A. L., & Pfahl, E. 2007, ApJ, 658, 1173
Popov, S., Blaschke, D., Grigorian, H., & Prokhorov, M. 2007, Ap&SS, 308, 381
Radice, D., Perego, A., Bernuzzi, S., & Zhang, B. 2018, MNRAS, 481, 3670
Rastinejad, J. C., Fong, W., Levan, A. J., et al. 2024, ApJ, 968, 14
Rice, W. K. M., Lodato, G., & Armitage, P. J. 2005, MNRAS, 364, L56
Shakura, N. I., & Sunyaev, R. A. 1973, A&A, 500, 33
Siegel, D. M., Agarwal, A., Barnes, J., et al. 2022, ApJ, 941, 100
Siegel, D. M., Barnes, J., & Metzger, B. D. 2019, Natur, 569, 241
Silva, H. O., Sotani, H., & Berti, E. 2016, MNRAS, 459, 4378
Stone, N. C., Metzger, B. D., & Haiman, Z. 2017, MNRAS, 464, 946
Sukhbold, T., Ertl, T., Woosley, S. E., Brown, J. M., & Janka, H. T. 2016, ApJ, 821, 38
Suwa, Y., Yoshida, T., Shibata, M., Umeda, H., & Takahashi, K. 2018, MNRAS, 481, 3305
Tauris, T. M., & Janka, H.-T. 2019, ApJL, 886, L20
Toomre, A. 1964, ApJ, 139, 1217
Woosley, S. E. 1993, ApJ, 405, 273
Woosley, S. E., & Bloom, J. S. 2006, ARAA, 44, 507
Woosley, S. E., Sukhbold, T., & Janka, H. T. 2020, ApJ, 896, 56